

Evidence of orographic precipitation suppression by air pollution induced aerosols in the western U.S.

Daniel Rosenfeld and Amir Givati

The Hebrew University of Jerusalem, Jerusalem, Israel

Corresponding author address:

Daniel Rosenfeld

Institute of Earth Sciences, The Hebrew University of Jerusalem
Jerusalem 91904, Israel.

Tel: Office: +972-2-6585821, Fax: +972-2-6512372

Email: Daniel.rosenfeld@huji.huji.ac.il

Submitted on 6 September 2005

Revision submitted on 3 November 2005

ABSTRACT

Analyses of trends of the orographic winter precipitation enhancement factor, R_o , along the coastal mountain ranges of the west coast of the USA show a pattern of decreasing R_o during the last century by as much as -24% from the southern border to central California, to no decrease in northern California and Oregon, and to a renewed decrease of R_o (-14%) in Washington to the Seattle area east of Puget Sound. Similar decreases occurred also well inland, over Arizona, New Mexico, Utah (this study) and the east (already documented earlier to this study) slopes of the Colorado Rockies. Both absolute precipitation amounts and R_o are affected by fluctuations in the atmospheric circulation patterns such as those associated with the Pacific Decadal Oscillation and the Southern Oscillation Index. However, these climatic fluctuations can not explain the observed trends in R_o . Although the trends of aerosols are available only since 1988, aerosol measurements from the IMPROVE aerosol monitoring network show that negative trends in R_o are associated with elevated concentrations of fine aerosols (PM_{2.5}). The PM_{2.5} showed stability or some increase in the areas where their levels were elevated and decreasing trends of R_o were noted. Strong decreasing trends of the coarse aerosols (PM₁₀-PM_{2.5}) were noted especially in the areas with elevated levels of PM_{2.5}. The decreasing trend in coarse aerosols (the coarse aerosols may act to initiate and enhance precipitation) in conjunction with the constancy and/or increases of the small aerosols (small aerosols suppress precipitation), can explain the continuing losses of orographic precipitation during the last two decades despite the indicated improvement in the conventional air quality standards.

1. Introduction

It was recognized more than 40 years ago that continental clouds have larger “colloidal stability” than maritime clouds (Squires, 1958). Laboratory experiments of relevance to coalescence in clouds in cloud condensation nuclei (CCN) rich and lean environments (Gunn and Phillips, 1957), led to the suggestion that highly continental clouds, which form in a CCN rich atmosphere, would produce less precipitation. Smoke from burning vegetation as well as urban and industrial air pollution serve as small CCN that form large concentrations of small cloud droplets. This in turn suppresses the drop coalescence and the warm rain processes, as well as the ice precipitation (Rosenfeld, 2000, Borys et al., 2003, Andreae et al., 2004) and so prolongs the time required to convert the cloud water that exists in small drops into large hydrometeors that can precipitate. On the other hand, precipitation forming processes can be accelerated upon addition of large ($> 1 \mu\text{m}$) hygroscopic CCN. These CCN can occur naturally in the form of salt from sea spray (Rosenfeld et al., 2002), salty dust from desert playas (Rudich et al., 2002), air pollution emissions from paper mills (Eagen et al., 1974), or even artificial hygroscopic cloud seeding materials (Silverman, 2003).

Precipitation can be shut off completely due to high concentrations of small aerosols polluting clouds having top temperatures $> -10^{\circ}\text{C}$ (Rosenfeld, 1999 and 2000; Rosenfeld and Woodley, 2003). The suppression of the precipitation-forming processes does not necessarily lead always to a net reduction of precipitation. The delay of early precipitation in deep convective clouds with warm bases such as those that occur in the tropics and the southeast USA in the summer can lead to their invigoration and to overall additional precipitation (Andreae et al., 2004; Khain et al., 2005), mainly due

to the dynamic response of the cloud development to the delayed precipitation.

In orographic clouds the slowing of the conversion rate of cloud water into precipitation would be manifested as a net reduction of surface precipitation, because orographic clouds are often shallow and short lived due to their forced termination downwind of the ridge line. Borys et al., (2003) showed that the addition of as little as $1\text{-}\mu\text{g m}^{-3}$ of sulfate aerosols to a clean background can reduce the orographic snowfall rate in the Colorado Rocky Mountains by up to 50%, due to suppression of the riming of ice crystals with the smaller cloud droplets.

Suppression of orographic precipitation by anthropogenic aerosols is expected to be quite abundant, especially on the west coast of continents in the subtropics and mid-latitudes, where the precipitation over the hills is a major source for the scarce water there. Pristine air that comes from the ocean becomes polluted over the densely populated coastal plains before ascending over the hills downwind, where the pollution can have its detrimental effect on the precipitation. Givati and Rosenfeld (2004, 2005) related observed trends of decreasing orographic precipitation to the possible microphysical effects of pollution aerosols. They defined the suppression of orographic precipitation as a reduction in the orographic enhancement factor R_o , where R_o is defined as the ratio between the precipitation amounts in the hills to the precipitation in the upwind lowland. Givati and Rosenfeld (2004) quantified for the first time the rainfall losses over hills and mountains downwind of major coastal urban areas in California and Israel. The suppression rate was found to be 15 - 25% of the annual precipitation in hilly areas in California and Israel (Givati and Rosenfeld, 2004, 2005). They showed that the suppression occurred mainly in the relatively shallow

orographic clouds within the cold air mass of cyclones and not in warm air masses. The R_o time series for relatively pristine areas crosswind to the polluted areas did not show any trend with time, and so served as controls to the polluted areas. Furthermore, Givati and Rosenfeld (2005) showed that the clouds that were most susceptible to the detrimental effects of air pollution over the hills in northern Israel were also the clouds for which glaciogenic cloud seeding caused the greatest rain enhancement. Givati and Rosenfeld (2005) suggest that it is reasonable to expect that clouds that are most sensitive to rain suppression due to aerosols that slow the rate of conversion of cloud droplets into precipitation particles would be also the clouds that would react most positively to cloud seeding that accelerates that rate.

Griffith et al (2005) indicated similar reductions in mountainous precipitation in Utah and Nevada in a work that followed the approach utilized in the study of Givati and Rosenfeld (2004). They examined the ratio of winter precipitation between valleys to mountain precipitation downwind of the Salt Lake City/Provo metropolitan complex. The ratio of precipitation at mountain stations that are located in rural settings in Utah and Nevada remained stable (Griffith et al, 2005), supporting of the role of pollution aerosols in decreasing R_o over the mountains to the east of Salt Lake City. While the decreasing trends of R_o in Utah occurred on the western slopes in precipitation that fell during westerly wind flows, similar decreasing trends in R_o of up to 30% were noted on the eastern slopes of the Rocky Mountains during easterly flows, downwind of Denver and Colorado Springs (Jirak and Cotton, 2005). It is difficult to explain how a change in the atmospheric circulation patterns could explain the decreasing trends of the orographic enhancement factor during both westerly and easterly winds over the respectively facing slopes,

preferentially downwind of major urban areas. The temporal changes in aerosols remain the most plausible explanation.

With this background, the objectives of this study are

- To examine the suppressive effect of aerosols on precipitation on a larger scale than California or Israel by looking at the ratio between the precipitation amounts over the hills to the precipitation over the upwind lowland areas in the western U.S, from the Pacific coast inland to the Rocky Mountains.
- To account for any variability that might be due to climatic fluctuations of the atmospheric circulation patterns.
- To relate the indicated trends in precipitation to trends in aerosol properties.

2. The study areas and methodology

2.1 Measuring the precipitation ratio of hilly to plains gauges

Following the methodology of Givati and Rosenfeld (2004, 2005) pairs of hilly and plains rain gauges (or clusters of gauges) were chosen for different areas across the western U.S. In order to encompass the multi-decadal scales of the longest periods of climatic fluctuations, we concentrated on the pairs with the longest available records. In addition to the long record, we required that the precipitation be highly correlated between the two gauges and the precipitation at the higher elevation rain gauge be considerably greater than the precipitation at the low lying rain gauge. In addition, the low lying precipitation gauge should be upwind of the higher precipitation gauge in most circumstances. The high correlation is required for using the low stations to predict the “natural” rainfall in the hilly station. The large orographic

enhancement factor indicates that much of the rainfall at the high station is generated by the orographic uplift of the air that comes from the region represented by the upwind lower elevation station. For each pair of stations the trend of the ratio between the mountains and the plains was tested. This was done for both urban and rural pairs of rain stations. The nearby rural side wind lowland-hill ratios were used as control areas for the precipitation trend analysis of the urban pairs.

2.2 Population growth in western USA during the 20th century

Many counties in the mountainous areas of the western USA are experiencing rapid growth in population (Booth, 1999). The population of the Southwestern United States has increased by approximately 1,500% between 1900 and 1990, while the population of the United States as a whole has grown by just 225%. Arizona had the fastest growth in population of 2,880%, followed by Nevada and Utah. Maricopa County (Phoenix), Arizona, had a 100-year growth rate of 10,275%, with most of that growth occurring between 1960 and 1990 (Chourre and Wright, 1997). The four fastest growing states in the U.S Between 1990 to 2000 were Nevada (66.3% gain), Arizona (40%), Colorado (30.6%) and Utah (29.6%). The U.S total population growth in the same period was only 13.2% (U.S. Bureau of the Census, 2004). This trend continued also between 2000 to 2004 (U.S. Bureau of the Census, 2004).

2.3 Precipitation characteristics in the western USA

The main precipitation source in the western USA during the winter is storms coming from the Pacific Ocean with mainly westerly winds (Davis and Walker, 1992). Most of the precipitation falls on the windward slopes of mountain ranges. During summer the polar vortex contracts and the Pacific

high expands and moves northward. This limits frontal precipitation along the west coast but precipitation produced by local convection occurs in many areas well inland. The dominant circulation that creates summer precipitation is advection of air from the Gulf of Mexico, mostly during July and August which is called the "summer monsoon" (Davis and Walker, 1992). Because the character of the precipitation in the western USA is different between summer and winter the analysis was done separately for winter time series (October -May) and summer time series (June-September). We expected that the aerosols would affect the summer convective and the winter orographic precipitation differently. The thermally driven summer convective clouds are deeper and more long-lived than the winter orographic clouds, and therefore not as susceptible to the suppressive effects of small aerosols on the total precipitation amounts. Model simulations showed enhanced concentrations of small CCN would still reduce the precipitation amounts from cold based convective clouds, but the effect reverses for warm based clouds, which actually produce more precipitation when polluted due to the delay of the early warm rainout (Khain et al., 2005).

In this study we analyze pairs of upwind plain gauges vs. downwind hilly rain gauges in conjunction with the measured aerosols at the locations presented in Figure 1. Table 1 provides the details for those rain gauges and table 2 provides the locations of the IMPROVE aerosol monitoring stations used in this study.

3. Aerosol properties and trends

The underlying assumption of the previous studies (Givati and Rosenfeld, 2004 and 2005) was that the trend of R_o encompassed the period of main growth of the population, so that the overall emissions at the end of the period is larger than at the beginning of the measured period, not requiring necessarily a monotonic growth throughout the analysis period. Respectively, the overall precipitation suppression was evaluated as ending/starting values of R_o , as calculated using a simple linear regression line of R_o as a function of year. Air pollution indices showed recovery (decreasing trend) in California after the Clean Air Act was legislated in 1977, but R_o continued to decrease, and certainly did not show any recovery since then. Givati and Rosenfeld (2004) suggested that there has been no decrease in the concentrations of small CCN, which are responsible for the suppression of precipitation, and pointed out the large increase in diesel consumption as a possible source of increasing production of such aerosols.

The current study expands the scope to the whole western USA, to both pristine and polluted areas. Analyses of aerosol properties and trends are expanded to be correlated with the observed trends of precipitation, based on the Interagency Monitoring of Protected Visual Environments (IMPROVE) monitoring program. Aerosol mass concentrations and composition during the winter months (October-March) were obtained for the areas of interest for the period 1988-2003 (Data are available from the program web site at <http://vista.cira.colostate.edu/improve/>). The trends were calculated using the tool provided at the IMPROVE web site at <http://vista.cira.colostate.edu/views/web/AnnualSummaryDev/Trends.aspx>.

This tool provides quarter yearly averaged values of the parameters. The annual "winter" value is the average of the first and last quarters for that year. The trends of the mass concentration of the particles smaller than 2.5 μm (PM_{2.5}) and of the particles with 2.5 < diameter < 10 μm (PM_{10-PM2.5}) were calculated and presented in Fig. 2. In addition, the trends of the following components of the fine particles were plotted: combined ammonium nitrates and sulfates, combined elemental and organic carbon, and soil materials. It is assumed here that small CCN concentrations are correlated positively with the mass of the soluble fraction of the fine particles, and hence act to suppress precipitation. Small CCN concentrations are certainly positively correlated with the fine fraction of sulfates and nitrates, and likely so with the carbonatous aerosols after having time between emission to reaching the mountain ranges to chemically mature and develop some solubility. Soil particles constitute a small fraction of the fine particles, but probably a larger fraction of the coarse particles. No information is available in the IMPROVE data about the composition of the coarse fraction. However, even insoluble mineral particles can become hygroscopic by interacting with air pollution and getting coated with soluble materials such as sulfates, and so act to enhance precipitation (Levin et al., 1996).

The analyzed IMPROVE stations were selected based on the availability of the longest possible time series of aerosol measurements that are the geographically closest to represent the conditions at the higher elevation gauge of the rain gauge pairs. The location of the selected IMPROVE stations are shown in figure 1 and their details are summarized table 2. The average aerosol concentrations probably differ considerably from those actually interacting with the clouds over the topographical barriers. However, we can

assume that the levels and trends of the aerosol concentrations that interact with the clouds are correlated those measured at the IMPROVE stations.

According to Figure 2 the central Sierra Nevada (Sequoia and Yosemite, panels A and B in Fig. 2) are much more polluted than the northern Sierra (Lassen Volcano, panel C in Fig. 2), in line with the strong decreasing trends of R_o in the central Sierra, but not in the north, as reported by Givati and Rosenfeld (2004). Furthermore, while the coarse particles show a decreasing trend, the fine particles are stable at very high levels of $8.5 \mu\text{m m}^{-3}$ in Sequoia, mainly in the form of nitrates, sulfates and organic carbon. The fine particle mass is smaller in Yosemite, probably due to the higher elevation of the monitoring station, but still showing a strong increasing trend mainly due to organic carbon. The decreasing trend of coarse aerosols that can have an enhancing effect on precipitation works in the same direction as the increasing trend of the fine aerosols that suppress precipitation. Coarse aerosols mass concentrations are decreasing also in the pristine areas in northern California and Oregon (panels C-E in Figure 2), but their concentrations are much smaller than in the central Sierra (Panels A-B in Figure 2). The concentrations of the fine aerosols in these pristine areas is very small and yet slightly decreasing. These fine aerosols are primarily composed of organic carbon, probably from residential wood stove combustion. Farther north in the densely populated and industrial area of Puget Sound (Panel F of Figure 2) the air is polluted once more, with an increasing trend of the fine aerosols, mainly due to nitrates.

If these IMPROVE stations represent the conditions during orographic precipitation, it would be consistent with decreasing trends of orographic precipitation in central California, stability in northern California to central

Oregon, and then decreasing trends again in Washington to the east of the densely populated area of Seattle, around Puget Sound.

Panels H of Figure 2 shows that Lone Peak to the east of Salt Lake City has high concentrations of fine aerosols, with a slightly increasing levels due to nitrate and sulfate, along with decreasing trend of coarse aerosols. This is compatible with the reported strong decrease (-24% during 1949-2004) of orographic precipitation to the east of Salt Lake (Griffith et al., 2005). The much cleaner air to the west and to the south (Great Basin and Bryce Canyon, panels I and L in Fig. 2) is consistent with the reported stability of the orographic precipitation in these regions (Griffith et al., 2005).

4. Ro trend analysis for winter and summer precipitation

Figure 1 summarizes the results of the winter Ro trend analysis between hilly rain gauges vs. relatively lower gauges upwind, in different locations across the western USA. It can be seen in the figure that the Ro has decreased significantly over the years (The numbers in Figure 1 are ending / starting of the winter Ro as shown in the panels of Figure 3) in all the areas except for the pristine regions of northern California, Oregon, southern Idaho and central Utah (regions 8, 9, 10, 11 and 6 in figure 1). The full statistics for all the pairs are provided in Table 4. Winter is defined here as October to May. The Ro values do not change much (most Ro values increase slightly) When restricting "winter" to October to March, so that the IMPROVE aerosols and rain gauges pertain exactly to the same months.

Figure 3 shows the winter and the summer Ro trends for gauges located in the Phoenix area, AZ (*number 2 in Figure 3*), Albuquerque, NM (3), Salt Lake, UT (5), Levan, UT, (6) Steamboat Springs, CO (7) and Seattle, WA

(12). The trends for additional polluted areas in California can be found at Givati and Rosenfeld (2004). While the R_o for the winter orographic precipitation (shallow, short-lived clouds) is decreasing, the same pairs of gauges show almost a stable trend for the summer precipitation (deep convective, long-lived clouds). Those findings are in agreement with what we found for many clustered hilly vs. plains rain gauges in California and Israel (Givati and Rosenfeld, 2004, 2005). Here we can also see that suppression of winter orographic precipitation occurs not only when maritime air is polluted over coastal urban areas, but also hundreds of kilometers farther inland.

Table 4 provides the gauge details, correlations between the pairs / clusters of gauges and summaries the R_o trend analysis for all gauges from figure 1.

No seasonal separation was done in areas with little summer precipitation, such as California (marked with * in table 2).

5. Testing trends in climate indices as an alternative explanation for decreasing R_o

The most likely alternative explanation for the reduction in R_o is a decreasing trend in the cross-mountain component of the low tropospheric wind velocity and moisture flux during rain events. Givati and Rosenfeld (2004) applied a radiosonde regression model and found that the relevant meteorological conditions during rainy days did not change systematically over the years, and the observed trends in R_o are likely caused by non-meteorological reasons, such as anthropogenic air pollution. Precipitation in the western USA may also be subject to climatic fluctuations like the El Niño-Southern Oscillation index (SOI) (Allan et al. 1991) and its multidecadal counterpart, the PDO, Pacific decadal oscillation (Zhang, 1996; Mantua et

al. 1997). The Pacific Decadal Oscillation (PDO) Index is defined as the leading principal component of the North Pacific monthly sea surface temperature variability. The PDO is a long-lived El Niño-like pattern of Pacific climate variability. The SOI is defined as the normalized pressure difference between Tahiti and Darwin (Ropelewski and Jones, 1987). Figure 4 displays the winter values (October-April) of (A) the PDO (after Mantua, 1997) and (B) SOI from 1900 to 2003. It can be seen that during this period the PDO had 3 phases: positive (warm) phase from 1900 - 1944, negative (cold) phase from 1945 - 1975 and another positive phase since 1976.

Dettinger (2004) characterized the effects of the PDO and the SOI on the ratio of precipitation between mountains and plain areas in the California Sierra Nevada. During negative PDO and positive SOI the westerly wind component is stronger so that the mountain / plains orographic factor is higher than in the positive PDO phase (El Niño like). There is less overall precipitation in the negative PDO than in the positive PDO phase (Dettinger, 2004). Figure 5 displays the relations between the PDO and SOI to the ratio between Cuyamaca and San Diego (A and B), and between Miami and Phoenix (C and D). It can be seen that the Ro is weakly negatively correlated with the PDO and even more weakly with the SOI. These weak relations could still explain the indicated trends if the PDO and SOI would have large trend with time. But this is not the case, as shown in the next section.

In order to better understand the possible effects of those climate indices on the orographic precipitation in the western USA we analyzed the hill / plain Ro of precipitation with respect to the winter values of the PDO and SOI. Pairs of hill / plain gauges with the longest record were chosen to test the climate indices fluctuations through the whole century:

Figure 6 presents the Ro of annual precipitation between hilly to plain stations for 3 pairs of stations with the longest record available: Cuyamaca / San Diego (CA), Miami / Phoenix (AZ), Lake Spaulding / Eureka (CA). Pairs A and B are located downwind to urban areas, while pair C is located in relatively pristine areas. The Ro time series were tested with respect to three PDO states: (A) $PDO < -0.5$, (B) Neutral state of $-0.5 < PDO < 0.5$ and (C) $PDO > 0.5$. It can be seen in the figure that the Ro between Cuyamaca vs. San Diego and Miami vs. Phoenix decrease for all PDO states, while the Ro in the pristine area (Lake Spaulding vs. Ukiah) remains stable with time in all the phases. In the polluted areas suppression of orographic precipitation increases with time regardless of the PDO phases.

Figure 7 shows the same methodology but for the Ro of the station pairs with the longest records with respect to three SOI states, as was done for the PDO. It can be seen that as with the PDO (Figure 6), the Ro decreases during all SOI phases for the polluted pairs, but not for the relatively pristine one.

Tables 4 and 5 display the results of multiple linear regressions, where the precipitation amounts and in Ro are explained by variability in PDO, SOI and year as the three independent regression parameters. The dependent variables in the regressions were the individual precipitation in the hilly and plains rain gauges (see table 4) and the Ro of precipitation between those hilly to plains gauges (see table 5). It can be seen in table 4 that the PDO and the SOI do affect the precipitation amounts. For example, P values for the PDO effect on precipitation in San Diego and in Cuyamaca are 0.004 and 0.005. Nonetheless when we test the effect of the PDO and SOI not on the absolute precipitation amounts but on the ratio between them no significant effect is found. The only variable that has a significant effect on the ratio is the year.

The R_o decreases significantly over the years, even when the variability in PDO and SOI is taken into account by the multiple regression model. The "years" variable represents another change that occurs with time and affects R_o . With lack of any other alternative explanation that we are aware of, we suggest that the decreasing R_o with the years is likely the result of the increasing small CCN aerosols and possibly the decreasing of giant CCN in the form of coarse aerosols over the years.

6. Discussion and conclusions

In this study we expanded the analysis of the possible effects of air pollution on orographic precipitation from California to the whole western USA. Analyses of trends of the orographic enhancement factor, R_o , along the coastal mountain ranges of the whole west coast of the USA showed a pattern of decreasing R_o by as much as -24% from the south border to central California, no decrease in northern California to Oregon, and a renewed decrease (-14%) in Washington to the east of Puget Sound. Both absolute precipitation amounts and R_o are affected by fluctuations in the atmospheric circulation patterns such as those associated with the PDO and SOI. However, these climatic fluctuations could not explain the observed trends in R_o . A case in point is the decreasing trend of R_o in both the western (this study) and eastern (Jirak and Cotton, 2005) slopes of the Rockies. It is difficult to imagine a trend in the circulation patterns that would result in such a trend.

Aerosol measurements since 1988 from the IMPROVE aerosol monitoring network in the west coast mountain ranges show that the negative trends in R_o were associated with elevated concentrations of fine aerosols (PM_{2.5}). The PM_{2.5} showed stability or some increase in the areas where

their levels were elevated and decreasing trends of R_o were noted. That increase came mainly from increasing nitrates and organic carbon that over compensated the decreasing trends in sulfates. In any case, there is certainly no indication for a decrease in the fine aerosols at the more polluted areas during the last two decades, which at least correspond to the lack of recovery of the orographic precipitation in response to the recent efforts to reduce the air pollution.

Strong decreasing trends of the coarse aerosols (PM₁₀-PM_{2.5}) was noted especially in the areas with elevated levels of PM_{2.5}. Coarse aerosols may enhance precipitation if they act as giant CCN. This is likely the case when the coarse particles interact with polluted air and get coated with soluble materials such as sulfates (Levin et al., 1996). If so, a decreasing trend in the concentrations of the coarse aerosols, in conjunction with stable or increasing concentrations of the small aerosols, might explain the continued trend of orographic precipitation losses during the last two decades, despite the indicated decreases in PM₁₀, based on conventional air quality standards. It remains to be determined why coarse aerosols have been decreasing during the last two decades while fine aerosols remained stable or increased at the same time.

It has been assumed that air masses well inland would not be as pristine as those impacting the coastline during on-shore flow, and therefore the impacts of pollution aerosols on orographic precipitation well inland would be smaller. However, analyses of R_o over the inland mountains of the western USA all the way to the Rockies shows that large decreases of R_o occur there (-15% to -25%) in areas that are potentially affected by anthropogenic sources. The IMPROVE aerosol measurements show elevated levels of PM_{2.5} in the areas that experienced decreasing trends of R_o , such as those

to the east of Salt Lake, UT, Phoenix, AZ, and Albuquerque NM. Low aerosol levels were recorded in southwest Utah and Idaho where the R_o trends were stable. The extent of decrease in R_o at the northern Rockies is not certain due to the fact that the winters of 1998-2003 are responsible for most of the decrease (See Fig. 7A). The decrease in R_o is contributed by the much reduced values at Steamboat Springs with no obvious deviation at Hayden at the same time. No similar strong decrease in the recent years was indicated anywhere else in the gauges analyzed for this study. If R_o occurred at the northern Colorado Rockies really decreased, it was associated with rather low aerosol levels measured on Mount Zirkel. These low concentrations may reflect mainly the high altitude (3243 m) of the measuring station. Such low concentrations of $PM_{2.5}$ (averaging about $2 \mu m m^{-3}$) do not exclude the possibility of long range transport air pollution being responsible to the possible decrease in R_o . Measurements conducted on top of a nearby mountain of the same elevation (Borys et al., 2003) have shown that fine aerosols concentrations as low as $1 \mu m m^{-3}$ can cut by half the snow precipitation rate compared to pristine conditions. In any case, we should not expect a perfect match between the IMPROVE and rain gauge trends, because the IMPROVE aerosol data cover only the last two decades, whereas the trends in Mount Zirkel were contributed mainly from the previous decades.

Evidently, decreases in R_o occurred during winter orographic precipitation but not during convective summer precipitation over the same mountain ranges. This is in line with the expectation that aerosol-induced changes in the rate of the conversion of cloud water to precipitation would result in a respective net change of surface precipitation in shallow and short-

lived orographic clouds, but not necessarily so in deeper and longer living thermally driven convective clouds.

These reported findings suggest that anthropogenic air pollution has had a major impact on orographic precipitation well beyond the local scale of the pollution sources. It appears that air pollution suppresses much of the orographic precipitation over the western USA, which is responsible for most of the water resources in this semi arid part of the world. This is an issue with major economical and societal implications, not only to the USA but to many other densely populated parts of the world where the livelihood of the inhabitants depend on water from orographic precipitation, which might be compromised by the air pollution produced by the inhabitants. Examples of such densely populated semi arid areas that depend on orographic precipitation that is susceptible to air pollution produced by the local inhabitants include the Mediterranean basin, the West Coast of the United States, the Middle East, south east Asia and China, and the southeastern part of Australia.

Acknowledgements

The work described here was made possible in part by funding by the Public Interest Energy Research (PIER) Program of the California Energy Commission. The authors thank Dr. W. L. Woodley for valuable discussions and reviewing the manuscript.

References

- Allan, R.J., Nicholls, N., Jones, P.D. and Butterworth, I.J., 1991: A further extension of the Tahiti-Darwin SOI, early SOI results and Darwin pressure. *J. Climate*, **4**, 743-749.
- Andreae, M. O., Rosenfeld, D., P., Costa, A. A., Frank, G. P., Longo, K. M. and Silva-Dias, M. A. F., 2004: Smoking rain clouds over the Amazon. *Science*, **303**, 1337-1342.
- Borys, R.D., D. H. Lowenthal, S. A. Cohn, and W. O. J. Brown, 2003: Mountain and radar measurements of anthropogenic aerosol effects on snow growth and snowfall rate. *Geophys. Res. Lett.*, **30** (10), 1538, doi: 10.1029/2002GL016855.
- Booth, D.E., 1999: Spatial patterns in the economic development of the Mountain West. *Growth and Change*, **30** (3): 384-405.
- Chourre, M. and S. Wright, 1993 : Population Growth of the Southwest United States, 1900-1990, Workshop on Impact of climate change and land use in the southwestern United States, Human impacts on the landscape, *U.S. Geological Survey*, University of Arizona, September 3-5, 1997
- Davis, R.E., D.R. Walker, 1992: An Upper-Air Synoptic Climatology of the Western United States. *J. of Climate*. **5**, 1449-1467.
- Dettinger, M., K. Redmond, and D. Cayan, 2004: Winter Orographic Precipitation Ratios in the Sierra Nevada - Large-Scale Atmospheric Circulations and Hydrologic Consequences. *J. Hydromet.*, **5**, 1102-1116.
- Eagen, R. C., P. V. Hobbs, and L. F. Radke, 1974: Particle emissions from a large Kraft paper mill and their effects on the microstructure of warm clouds. *J. Appl. Meteor.*, **13**,(5):535-552.
- Givati, A. and D. Rosenfeld, 2004: Quantifying precipitation suppression due to air pollution. *J. Appl. Meteor.*, **43**, 1038-1056.

Givati, A. and D. Rosenfeld, 2005: Separation between cloud seeding and air pollution effects. *J. Appl. Meteor.*, in press.

Griffith, D.A., M.E. Solak and D.P. Yorty, 2005: Is Air Pollution Impacting Winter Orographic Precipitation in Utah? Weather Modification Association, *Journal of Weather Modification*, Vol. **37**, pp. 14-20.

Gunn, R. and B. B. Phillips, 1957: An experimental investigation of the effect of air pollution on the initiation of rain. *J. Meteor.*, **14**, 272-280.

Khain, A., D. Rosenfeld and A. Pokrovsky, 2005: Aerosol impact on the dynamics and microphysics of convective clouds. *The Quarterly Journal of the Royal Meteorological Society*. In Press.

Jirak, I. L., and W.R. Cotton, 2005: Effect of Air Pollution on Precipitation along the Front Range of the Rocky Mountains, *J. Appl. Meteor.*, in press.

Levin, Z., E. Ganor, V. Gladstein, 1996: The Effects of Desert Particles Coated with Sulfate on Rain Formation in the Eastern Mediterranean. *J. Appl. Meteor.* **35**, 1511-1523

Mantua, N.J., S.R. Hare, Y. Zhang, J.M. Wallace, and R.C. Francis, 1997: A Pacific interdecadal climate oscillation with impacts on salmon production. *Bull. Amer. Meteor. Soc.*, **78**, 1069-1079.

Ropelewski, C.F. and P.D., Jones, 1987: An extension of the Tahiti-Darwin Southern Oscillation Index. *Monthly Weather Review* ,**115**, 2161-2165

Rosenfeld, D., 1999: TRMM observed first direct evidence of smoke from forest fires inhibiting rainfall. *Geophys. Res. Lett* , **26**, 3105-3108 .

Rosenfeld, D., 2000: Suppression of rain and snow by urban air pollution. *Science*, **287**, 1793-1796.

Rosenfeld, D. and W. L. Woodley, 2003: Closing the 50-year circle: From cloud seeding to space and back to climate change through precipitation

physics. Chapter 6 of "Cloud Systems, Hurricanes, and the Tropical Rainfall Measuring Mission (TRMM)" edited by Drs. Wei-Kuo Tao and Robert Adler, 234pp., *Meteorological Monographs*, **51**, 59-80, AMS.

Rosenfeld, D., R. Lahav, A. P. Khain, M. Pinsky, 2002: The role of sea-spray in cleansing air pollution over ocean via cloud processes. "Research Article" in *Science*, **297**, 1667-1670.

Rudich, Y., D. Rosenfeld, O. Khersonsky, 2002: Treating clouds with a grain of salt. *Geophys. Res. Lett.*, **29** (22), doi:10.1029/2002GL016055, 2002.

Silverman, B. A., 2003: A critical assessment of hygroscopic seeding of convective clouds for rainfall enhancement. *Bull. Amer. Meteor. Soc.*, **84**, 1219-1230

Squires, P., 1958: The microstructure and colloidal stability of warm clouds. *Tellus* **10**, 256-271.

U.S. Bureau of the Census, 2004: Selected Historical Decennial Census Population and Housing Counts, <http://www.census.gov/popest/states/NST-pop-chg.html>.

U.S. Bureau of the Census, 2004: Population estimates, National and state population estimates, <http://www.census.gov/popest/states/tables/NST-EST2004-02.xls>.

Zhang, Y., J.M. Wallace, D.S. Battisti, 1997: ENSO-like interdecadal variability: 1900-93. *J. Climate*, **10**, 1004-1020.

Figure captions

Figure 1: Summary map of the locations of the rain gauges, aerosol monitoring stations and the main results of the orographic precipitation. Rain gauge pairs are marked by the blue circle for the low station and red circle for the downwind hilly station. Clusters of gauges are shown by an irregular enclosure. The station pairs are numbered and the respective details are provided in Table 1. The fractional change of the winter (October-May) orographic enhancement factor of the high rain gauge(s) with respect to the low rain gauge(s) that was indicated during the measurement period is shown near each pair. The red numbers are smaller than 1.00 with statistical significance of $P < 0.05$. P is the statistical significance that corresponds to the t test statistic, which measures the probability that there is no trend. The locations of the IMPROVE aerosol monitoring stations are shown in the yellow circles and marked by characters respective to the reference in the text and the station details in Table 2.

Figure 2: Trends of coarse ($2.5 < \text{diameter} < 10 \mu\text{m}$) and fine ($\text{Diameter} < 2.5 \mu\text{m}$) aerosols mass concentrations and compositions as measured during winter (October-March) by the IMPROVE monitoring program. The mass concentrations are given in $\mu\text{g m}^{-3}$. The composition of the fine aerosols is divided into mass of nitrates and sulfates ($\text{SO}_4 + \text{NO}_3$), organic and elemental carbon (Carbon) and crustal materials (Soil). The legend is provided at the top of the figure. The locations of the stations are marked with the respective letter on the map in Fig. 1, and tabulated in Table 1.

Figure 3: Trend analysis for winter and summer ratio of precipitation measured in cluster of gauges in: Phoenix area vs. downwind hilly cluster of gauges (2A and 2B), Albuquerque and Sandia crest (3A,3B), cluster of gauges in Salt Lake City and in downwind hilly cluster of gauges (5A,5B), Levan vs. Delta (6A,6B), Steamboat vs.

Hayden (7A,7B) and cluster of gauges in Seattle area vs. the downwind hilly gauge Palmer (12A,12B). Note the sharp decrease in Ro of winter precipitation with time in areas which are affected by urban air pollution, while the Ro of summer precipitation remains stable.

Figure 4: winter values (October - April) of the PDO and SOI indexes. Note the three phases of the PDO: positive from 1900 - 1944, negative phase from 1945 - 1975 and another positive phase since 1976.

Figure 5: The relations between the PDO and SOI to the orographic enhancement factor (Ro) between Cuyamaca and San Diego (A and B), and between Miami and Phoenix (C and D). Note the low correlation between the PDO and SOI to Ro.

Figure 6: PDO classification to three states and the ratio of hilly / plain pairs of rain gauges in polluted areas (Cuyamaca / San Diego, Miami / Phoenix) and relatively pristine area (Lake Spalding / Ukiah). The ratio for the polluted pairs decreases in all PDO states, while no trend is indicated for the ratio at the relatively pristine area.

Figure 7: Same as Figure 6 but for SOI classification to three states. As in Fig. 6, the ratio for the polluted pairs decreases in all SOI states, while no trend is indicated for the ratio in the relatively pristine area.

Set of Figures

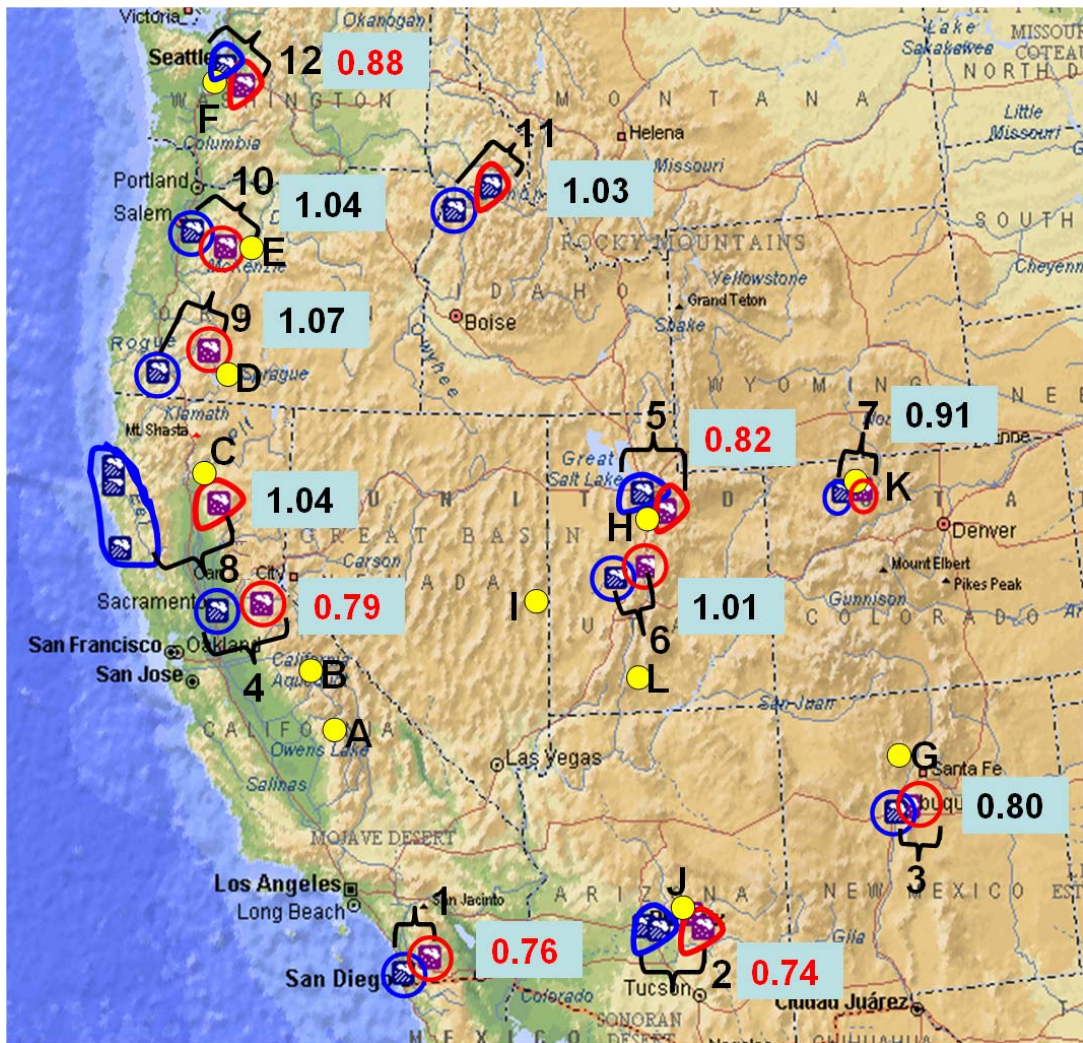


Figure 1: Summary map of the locations of the rain gauges, aerosol monitoring stations and the main results of the orographic precipitation. Rain gauge pairs are marked by the blue circle for the low station and red circle for the downwind hilly station. Clusters of gauges are shown by an irregular enclosure. The station pairs are numbered and the respective details are provided in Table 1. The fractional change of the winter (October-May) orographic enhancement factor of the high rain gauge(s) with respect to the low rain gauge(s) that was indicated during the measurement period is shown near each pair. The red numbers are smaller than 1.00 with statistical significance of $P < 0.05$. P is the statistical significance that corresponds to the t test statistic, which measures the probability that there is no trend. The locations of the IMPROVE aerosol monitoring stations are shown in the yellow circles and marked by characters respective to the reference in the text and the station details in Table 2.

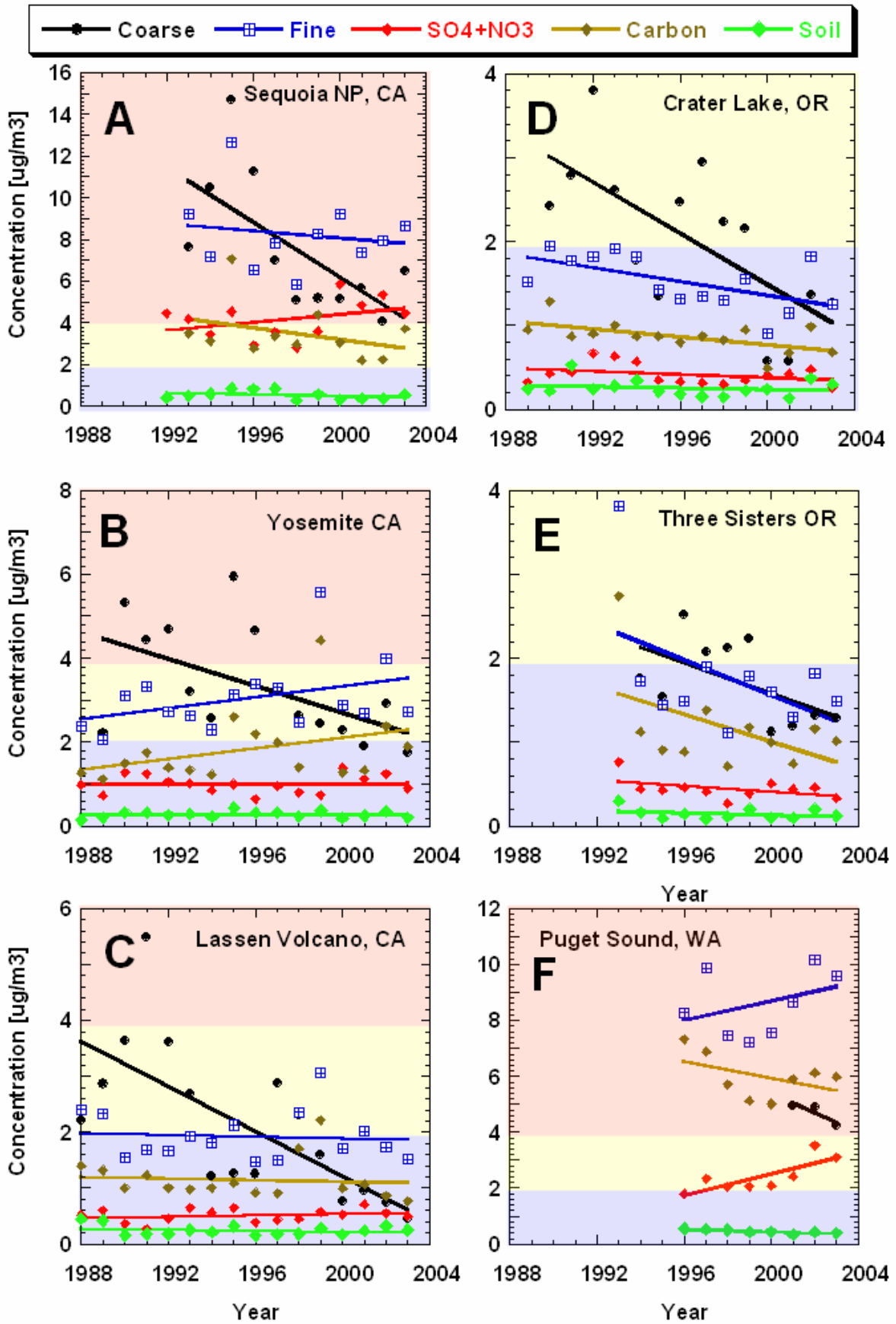


Figure 2 (page 1/2)

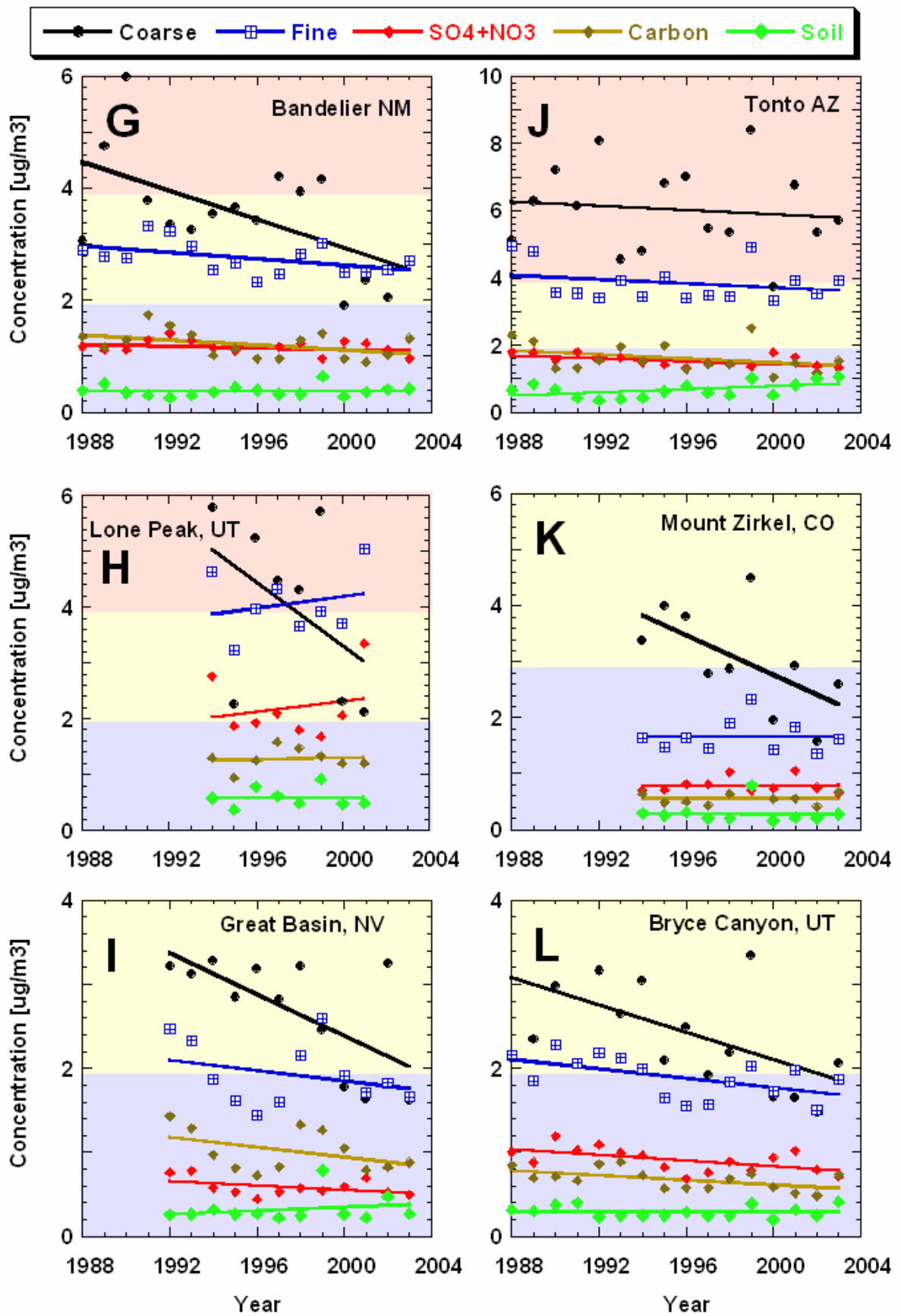


Figure 2 (page 2/2)

Figure 2: Trends of coarse ($2.5 < \text{diameter} < 10 \mu\text{m}$) and fine ($\text{Diameter} < 2.5 \mu\text{m}$) aerosols mass concentrations and compositions as measured during winter (October-March) by the IMPROVE monitoring program. The mass concentrations are given in $\mu\text{g m}^{-3}$. The composition of the fine aerosols is divided into mass of nitrates and sulfates ($\text{SO}_4 + \text{NO}_3$), organic and elemental carbon (Carbon) and crustal materials (Soil). The legend is provided at the top of the figure. The locations of the stations are marked with the respective letter on the map in Fig. 1, and tabulated in Table 1.

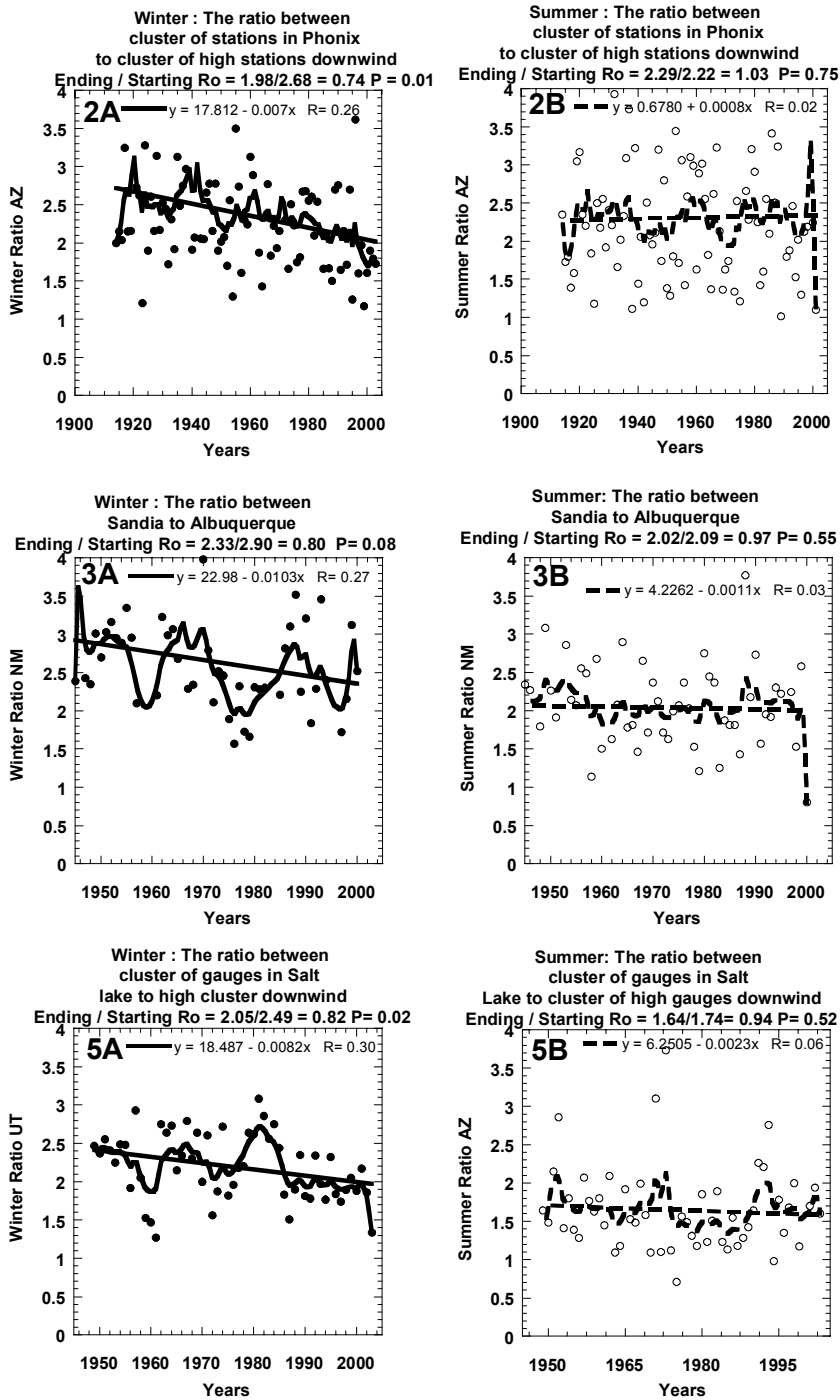


Figure 3 (page 1/2)

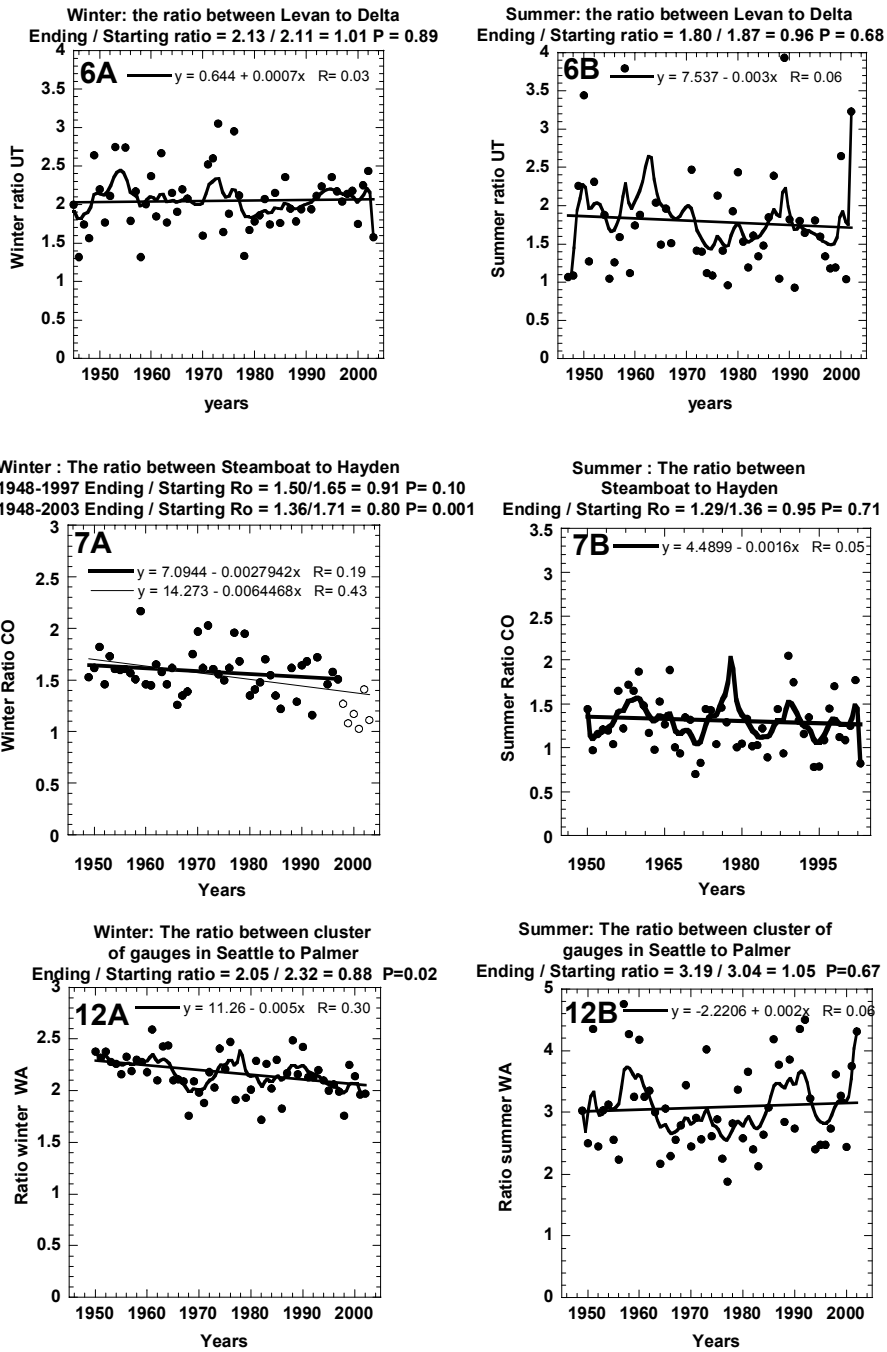


Figure 3 (page 2/2)

Figure 3: Trend analysis for winter and summer ratio of precipitation measured in cluster of gauges in: Phoenix area vs. downwind hilly cluster of gauges (2A and 2B), Albuquerque and Sandia crest (3A,3B), cluster of gauges in Salt Lake City and in downwind hilly cluster of gauges (5A,5B), Levan vs. Delta (6A,6B), Steamboat vs. Hayden (7A,7B) and cluster of gauges in Seattle area vs. the downwind hilly gauge Palmer (12A,12B). Note the sharp decrease in Ro of winter precipitation with time in areas which are affected by urban air pollution, while the Ro of summer precipitation remains stable.

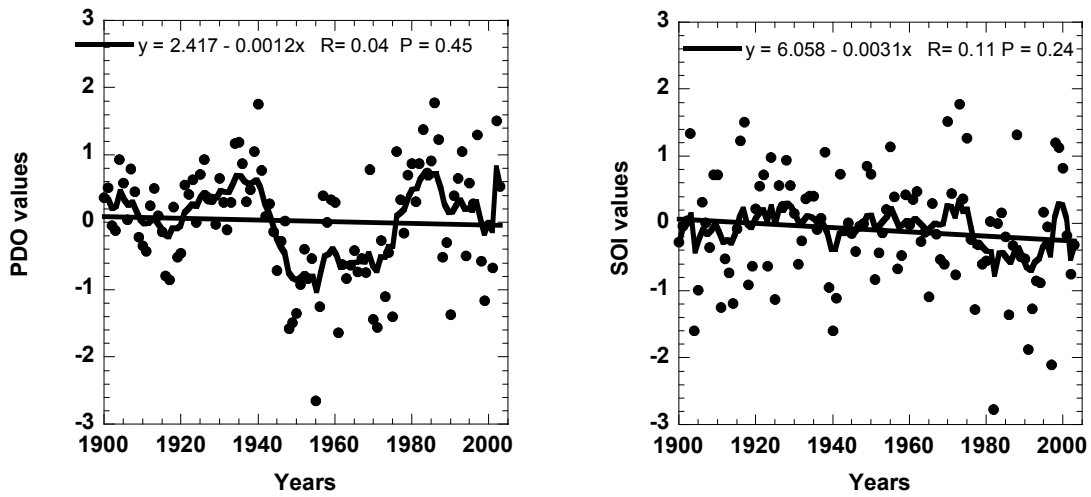


Figure 4: winter values (October - April) of the PDO and SOI indexes. Note the three phases of the PDO: positive from 1900 - 1944, negative phase from 1945 - 1975 and another positive phase since 1976.

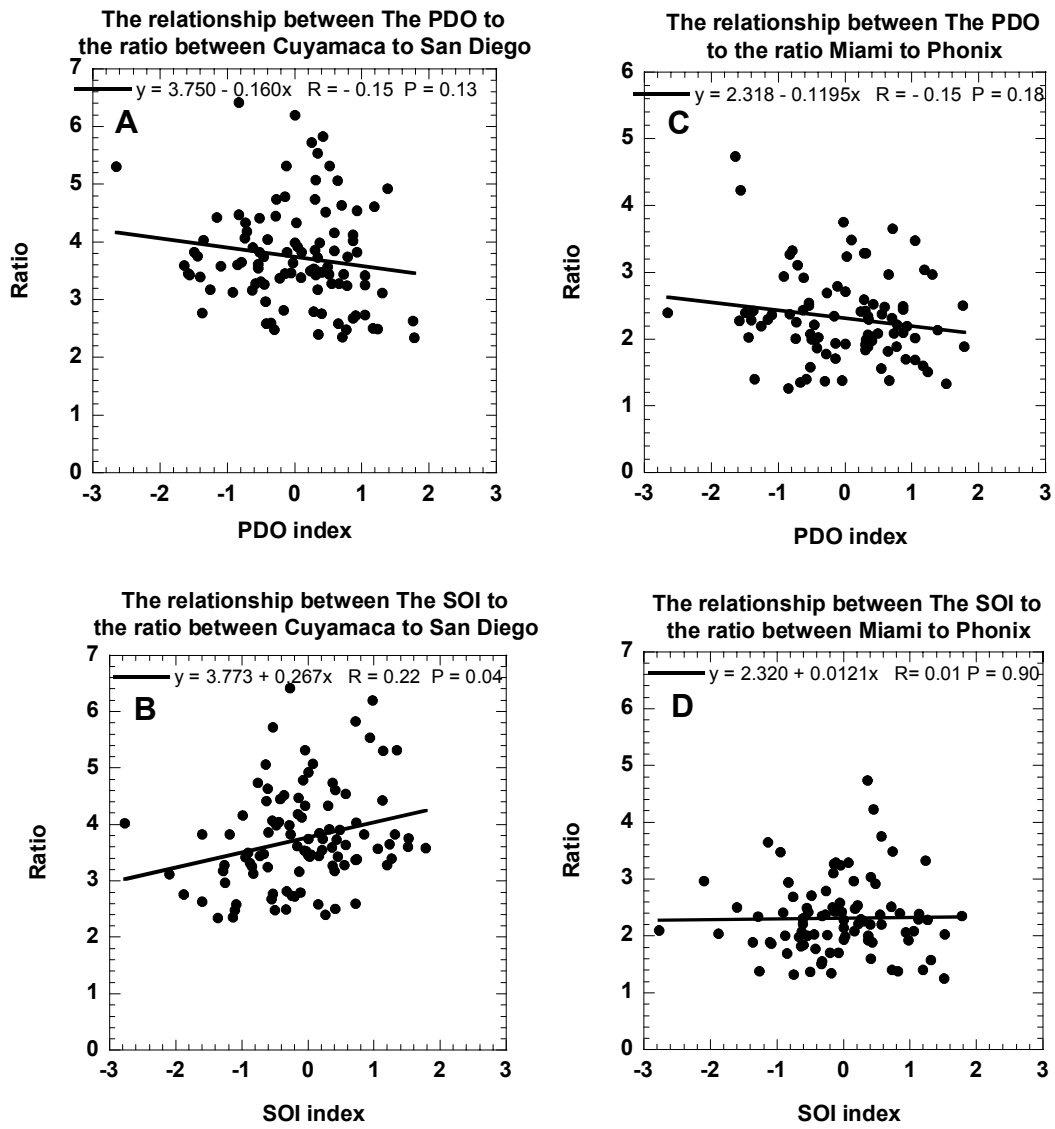


Figure 5: The relations between the PDO and SOI to the orographic enhancement factor (Ro) between Cuyamaca and San Diego (A and B), and between Miami and Phoenix (C and D). Note the low correlation between the PDO and SOI to Ro.

PDO < -0.5

-0.5 < PDO < 0.5

PDO > 0.5

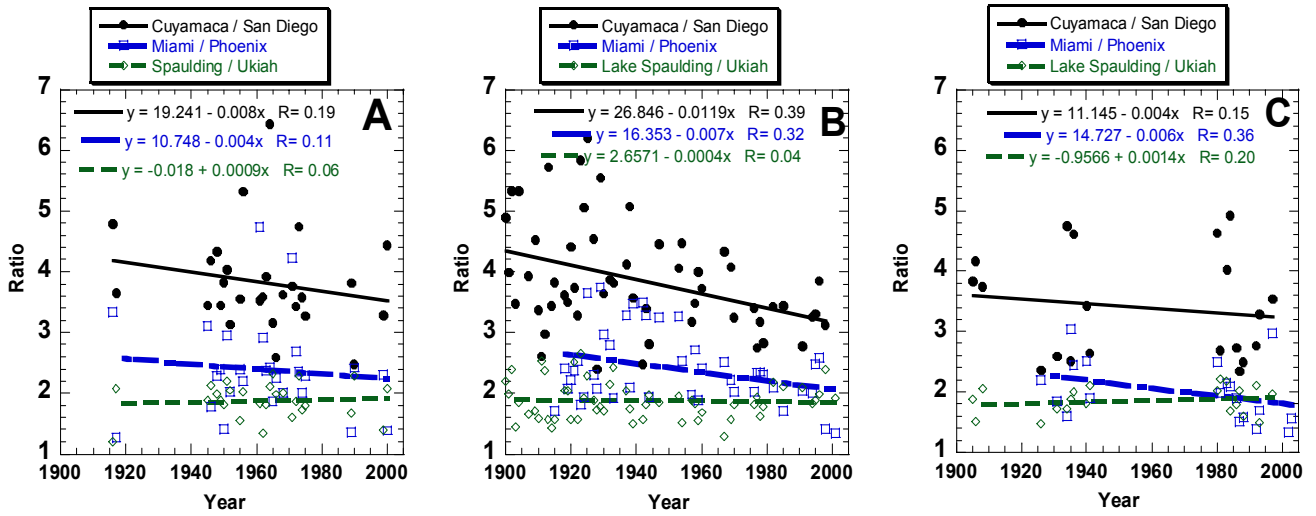


Figure 6: PDO classification to three states and the ratio of hilly / plain pairs of rain gauges in polluted areas (Cuyamaca / San Diego, Miami / Phoenix) and relatively pristine area (Lake Spaulding / Ukiah). The ratio for the polluted pairs decreases in all PDO states, while no trend is indicated for the ratio at the relatively pristine area.

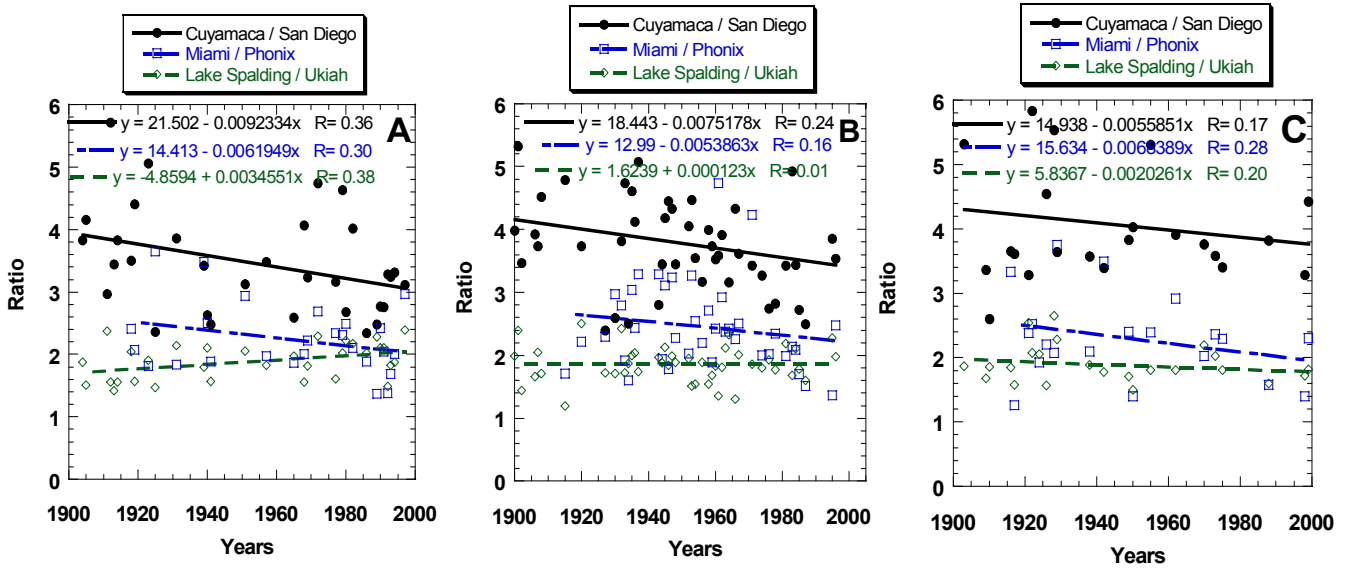


Figure 7: Same as Figure 6 but for SOI classification to three states. As in Fig. 6, the ratio for the polluted pairs decreases in all SOI states, while no trend is indicated for the ratio in the relatively pristine area.

Tables

Table 1: The locations and details of the plains and hilly rain gauge pairs and clusters, as numbered in figure 1. Clusters of gauges appear under the same pair number.

Pair No.	Data since	State	Plains stations	Lat	Long	Elev(m)	Hilly stations	Lat	Long	Elv(m)
1	1888	CA	San Diego	32.44	-117.10	10	Cuyamaca	32.59	-116.35	1557
2	1914	AZ	Litchfield park	33.30	-11.222	343	Miami	33.24	-110.53	1200
2		AZ	Sacaton	33.05	-111.45	427	Roosevelt	33.40	-111.09	733
2		AZ	Mesa	33.25	-111.52	410				
2		AZ	Goulds ranch	33.23	-112.04	400				
3	1945	NM	Albuquerque	35.03	-106.37	1770	Sandia crest	35.13	-106.27	3563
4	1945	CA	Sacramento	38.31	-121.30	8	Pacific House	38.75	-12.050	1147
5	1949	UT	Tooele	40.32	-112.18	1607	Silver lake	40.36	-111.35	2903
5		UT	Salt Lake/Garfield	40.43	-112.12	1437	Alta	40.36	-111.38	2903
5		UT					Cottonwood	40.37	-111.47	1653
6	1945	UT	Delta	39.23	-112.31	1587	Levan	39.33	-111.52	1770
7	1948	CO	Hayden	40.29	-107.15	2127	Steamboat Springs	40.30	-106.50	2257
8	1949	CA	Eureka	40.48	-124.10	3	Mineral	40.35	-121.600	1627
8		CA	Scotia	40.29	-124.06	5	De Sabla	39.52	-121.370	907
8		CA	Fort Bragg	39.27	-123.48	3				
9	1949	OR	Grant pass	42.26	-123.19	310	Crater lake	42.54	-122.08	2160
10	1954	OR	Stayton	44.48	-122.46	157	Marion forks	44.37	-121.57	817
11	1958	ID	Riggins Ranger	45.25	-116.19	600	Elk city	45.49	-115.26	1327
							Headquarters	46.38	-115.48	1047
12	1949	WA	Seattle	47.36	-122.20	3	Palmer	47.18	-121.50	300
12		WA	Kent	47.23	-122.14	10				
12		WA	Puyallup	47.12	-122.20	17				

Table 2: The locations of the IMPROVE aerosol monitoring stations used in this study.

Station	State	ID code	Site Name	Latitude	Longitude	Elev (m)
A	CA	SEQU1	Sequoia	36.489	-118.829	519
B	CA	YOSE1	Yosemite	37.712	-119.704	1603
C	CA	LAVO1	Lassen	40.540	-121.578	1732
D	OR	CRLA1	Crater Lake	42.896	-122.136	1966
E	OR	THSI1	Three Sisters	44.291	-122.043	885
F	WA	PUSO1	Puget Sound	47.570	-122.312	97
G	NM	BAND1	Bandelier	35.78	-106.266	1988
H	UT	LOPE1	Lone Peak	40.445	-111.708	1768
I	NV	GRBA1	Great Basin	39.005	-114.216	2065
J	AZ	TONT1	Tonto	33.649	-111.109	775
K	CO	MOZI1	Mount Zirkel	40.538	-106.677	3243
L	UT	BRCA1	Bryce Canyon	37.618	-112.174	2481

Table 3: P values and the regression equations for the IMPROVE aerosol trends

Site Name	Sequoia	Yosemite	Lassen	Crater Lake	Three Sisters	Puget Sound
Station	A	B	C	D	E	F
Coarse P value	0.02	0.03	0.002	0.006	0.04	0.29
Coarse equation	$y = -0.6587x + 1322.7$	$y = -0.1599x + 322.4$	$y = -0.2007x + 402.65$	$y = -0.1522x + 305.82$	$y = -0.0919x + 185.4$	$-0.3475x + 700.38$
Fine P value	0.63	0.16	0.73	0.008	0.12	0.36
Fine equation	$Y = -0.0882x + 184.44$	$Y = 0.0883x - 173.1$	$y = -0.0084x + 18.703$	$y = -0.0428x + 86.931$	$y = -0.1051x + 211.74$	$y = 0.1753x - 341.91$
SO4+NO3 P value	0.13	0.83	0.98	0.46	0.13	0.01
SO4+NO3 equation	$y = 0.1423x - 280.12$	$y = 0.0061x - 11.071$	$y = 0.0062x - 11.926$	$y = -0.005x + 10.419$	$y = -0.0182x + 36.774$	$y = 0.1921x - 381.64$
Carbon P value	0.29	0.16	0.71	0.003	0.13	0.24
Carbon equation	$y = -0.1413x + 285.84$	$y = 0.075x - 147.88$	$y = -0.0077x + 16.606$	$y = -0.0306x + 61.998$	$y = -0.0815x + 163.91$	$y = -0.15x + 305.93$
Soil P value	0.12	0.49	0.33	0.60	0.33	0.01
Soil equation	$y = -0.0322x + 64.854$	$y = 0.0045x - 8.6615$	$y = -0.0049x + 10.064$	$y = -0.003x + 6.1666$	$y = -0.0063x + 12.682$	$y = -0.0246x + 49.73$
Site Name	Bandelier	Lone Peak	Great Basin	Tonto	Mount Zirkel	Bryce Canyon
Station	G	H	I	J	K	L
Coarse P value	0.01	0.27	0.02	0.66	0.07	0.04
Coarse equation	$-0.1273x + 257.48$	$y = -0.286x + 575.21$	$y = -0.1225x + 247.36$	$y = -0.0317x + 69.35$	$y = -0.1773x + 357.43$	$y = -0.0809x + 164$
Fine P value	0.07	0.59	0.34	0.30	0.94	0.02
Fine equation	$-0.0278x + 58.306$	$y = 0.0536x - 103.07$	$y = -0.0311x + 64.023$	$y = -0.0321x + 67.973$	$y = 0.0025x - 3.357$	$y = -0.028x + 57.816$
SO4+NO3 P value	0.26	0.62	0.15	0.02	0.89	0.02
SO4+NO3 equation	$-0.008x + 17.122$	$y = 0.0484x - 94.474$	$y = -0.0128x + 26.185$	$y = -0.0209x + 43.291$	$y = 0.0023x - 3.7425$	$y = -0.0171x + 35.025$
Carbon P value	0.08	0.80	0.17	0.18	0.81	0.02
Carbon equation	$-0.0224x + 46.014$	$y = 0.0081x - 14.888$	$-0.0288x + 58.567$	$y = -0.0309x + 63.333$	$y = 0.0032x - 5.9135$	$y = -0.0142x + 28.955$
Soil P value	0.67	0.87	0.46	0.05	0.88	0.84
Soil equation	$y = 0.0023x - 4.1211$	$y = 0.003x - 5.3562$	$y = 0.0105x - 20.629$	$y = 0.0239x - 47.041$	$y = -0.0032x + 6.7094$	$y = -0.0008x + 1.8509$

Table 4: Rain gauge details and summary of the Ro trend analysis for winter and summer precipitation. See Explanation for the table's entries below the table.

Stations name¹	1 San Diego	1 Cuyamaca	2 Phoenix cluster	2 cluster downwind to Phoenix	3 Albuquerque	3 Sandia
State	CA	CA	AZ	AZ	NM	NM
Long / Lat² [Decimal]	-117.10/ 32.44	-116.36/ 32.59	-111.80/ 33.20	-111.22/ 33.30	-106.37/ 35.03	-106.27/ 35.13
Years³	1888 - 2003		1914 - 2003		1945 - 2000	
Elevation⁴ [m]	3	1550	395	970	1170	3563
Average winter precip. [mm]⁵	290*	875*	130	283	107	254
Average summer precip. [mm]⁵			80	164	123	246
Correlation winter⁶	0.80		0.89		0.82	
Correlation summer⁶			0.69		0.61	
Ending/Starting ratio winter⁷	3.28 / 4.32 = 0.76		1.98/2.68 = 0.74		2.33 / 2.90 = 0.80	
Ending/Starting ratio summer⁷			2.29/2.22 = 1.03		2.02/2.09 = 0.97	
P value winter⁸	P = 0.003		P = 0.01		0.08	
P value summer⁸			P = 0.75		0.55	
Equation winter⁹	y = 20.871 - 0.008x		y = -0.0079x + 17.81		y = -0.0103x + 22.938	
Equation summer			y = 0.6780 + 0.00082x		y = 4.223 + 0.001x	
Stations name	4 Sacramento	4 Pacific House	5 Salt Lake cluster low	5 cluster downwind to Salt Lake	7 Hayden	7 Steamboat Spring
State	CA	CA	UT	UT	CO	CO
Long / Lat [Decimal]	-121.30/ 38.35	-120.50/ 38.750*	-112.15/ 40.37	-111.40/ 40.36	-107.15/ 40.29	-106.50/ 40.30
Years	1945 - 2002		1949 - 2003		1948 - 2002 / 1997	
Elevation [m]	8	1147	1521	2487	2126	2257
Average winter precip. [mm]	475*	1321*	342	748	292	445
Average summer precip. [mm]			152	227	170	209
Correlation winter	0.86		0.79		0.80	
Correlation summer			0.84		0.85	
Ending/Starting ratio winter	2.48 / 3.15 = 0.79		2.05 / 2.49 = 0.82		1948-1997: 1.50 / 1.65 = 0.91 1948-2002: 1.36 / 1.71 = 0.80	
Ending/Starting ratio summer			1.64 / 1.74 = 0.96		1.29 / 1.36 = 0.95	
P value winter	0.003		0.02		0.001 / 0.10	
P value summer			0.52		0.71	
Equation winter	y = 35.863 - 0.017x		y = 18.487 - 0.0082x		y = 14.273 - 0.0064x	
Equation summer			y = 6.2504 - 0.0023x		y = 4.899 + 0.0016x	

Stations name¹	6 Levan	6 Delta	12 Seattle cluster low	12 Palmer	8 Northern CA cluster	8 Northern CA cluster downwind
State	UT	UT	WA	WA	CA	CA
Long / Lat² [Decimal]	-112.31/ 39.23	-111.52/ 39.33	-122.20/ 47.36	-121.50/ 47.18	-123.88/ 40.01	-121.48/ 38.583
Years³	1945-2003		1949-2003		1949-2000	
Elevation [m]⁴	1585	1770	10	300	3	1270
Average winter⁵ precip. [mm]	280	144	812	1734	1090	1550
Average summer precip. [mm]	90	54	127	381		
Correlation winter⁶	0.85		0.89		0.90	
Correlation summer	0.79		0.83			
Ending/Starting ratio winter⁷	2.13 / 2.11 = 1.01		2.05 / 2.32 = 0.88		1.43 / 1.37 = 1.04	
Ending/Starting ratio summer	1.80 / 1.87 = 0.96		3.19 / 3.04 = 1.04			
P value winter⁸	0.89		0.02		0.57	
P value summer	0.68		0.67			
Equation winter⁹	y = 0.644 + 0.0007x		y = 11.26 - 0.005x		y = 0.0011x - 0.6877	
Equation summer	y = -0.0026x + 7.537		y = -2.226x + 0.00X			
Stations name	9 Grants Pass	9 Crater Lake	10 Stayton	10 Marion	11 Riggins	11 Cluster High
State	OR	OR	OR	OR	ID	ID
Long / Lat [Decimal]	-123.19/ 42.26	-122.08/ 42.54	-122.46/ 44.48	-121.57/ 44.37	-116.19/ 45.25	-115.37/ 45.93
Years	1949-2003		1954-2002		1958-2003	
Elevation [m]	310	2160	600	1187		
Average yearly precip. [mm]	767	1682	422	860		
Correlation⁶	0.86		0.91		0.70	
Ending/Starting ratio	2.25 / 2.10 = 1.07		1.39/1.34 = 1.04		2.17/2.11 = 1.03	
P value	0.29		0.20		0.77	
Equation	y = -3.7154 + 0.0029x		y = -1.3998 + 0.00134x		y = -0.2165 + 0.001x	

Explanation for the Table 4 entries:

- 1. Stations / Cluster name:** The rain gauge name or the cluster name, and the pair number as appearing on Figure 1.
- 2. Long / Lat:** The geographical longitude and latitude [in decimal degrees].
- 3. Years:** the period of precipitation measurements.
- 4. Elevation:** The elevation of the rain gauges in meters above sea level.
- 5. Average winter / summer precip. :** The average amount of precipitation at each station for winter period (October - May) and the summer (June - September) in [mm/year].
- 6. Correlation:** the correlation for the winter or the summer precipitation between the plains to the hilly gauge readings.

7. Ending / Starting ratio: The ratio (where the ratio is defined as the ratio between the precipitation amounts at the hills and at the upwind lowland) in the beginning of the time series compared to the ratio at the end of the time series the change, as calculated using the regression line. This is the trend along the years.

8. P value: The statistical significance of the trend corresponds to the t test statistic. It quantifies the chance that there is no trend.

9. Regression equation: The regression equation used to calculate the trend.

Table 4: Multiple linear regression results showing the significances of three independent variables: The PDO, the SOI and the years, vs. the dependent variable - individual precipitation of rain gauges across the U.S.

Station Name	San Diego	Cuyamaca	Sacramento	Pacific H.	Phoenix Cluster	Cluster downwind to Phoenix
State	CA	CA	CA	CA	AZ	AZ
PDO P value	0.004	0.005	0.642	0.358	0.254	0.253
SOI P value	0.43	0.175	0.247	0.972	0.001	0.001
Years P value	0.522	0.287	0.580	0.835	0.423	0.064
Station Name	Albuq.	Sandia	Salt Lake Cluster	Cluster downwind to Salt Lake	Hayden	Steamboat
State	NM	MN	UT	UT	CO	CO
PDO P value	0.558	0.970	0.541	0.528	0.479	0.851
SOI P value	0.112	0.007	0.461	0.539	0.576	0.820
Years P value	0.006	0.005	0.037	0.519	0.580	0.588
Station/s Name	Seattle cluster	Palmer				
State	WA	WA				
PDO P value	0.004	0.072				
SOI P value	0.564	0.923				
Years P value	0.221	0.080				

Table 5: Multiple linear regression results showing the significance of three independent variables: The PDO, the SOI and years, vs. the dependent variable - ratio of precipitation between the rain gauge pairs, which is the orographic enhancement factor, Ro.

Pairs of stations	Cuyamaca / San Diego	Pacific H. / Sacramento	Phoenix Cluster / Cluster down wind	Albuq. /Sandia	Salt L .City Cluster / Cluster down wind	Steamboat/ Hayden	Seattle cluster/ Palmer
State	CA	CA	AZ	NM	UT	CO	WA
PDO P value	0.430	0.431	0.478	0.577	0.911	0.110	0.394
SOI P value	0.100	0.703	0.703	0.451	0.840	0.216	0.419
Years P value	0.005	0.012	0.010	0.153	0.050	0.083	0.0001